

This is the accepted manuscript made available via CHORUS. The article has been published as:

Theoretical investigation of the evolution of the topological phase of $\text{Bi}_{\{2\}}\text{Se}_{\{3\}}$ under mechanical strain

Steve M. Young, Sugata Chowdhury, Eric J. Walter, Eugene J. Mele, Charles L. Kane, and
Andrew M. Rappe

Phys. Rev. B **84**, 085106 — Published 19 August 2011

DOI: [10.1103/PhysRevB.84.085106](https://doi.org/10.1103/PhysRevB.84.085106)

Theoretical investigation of the evolution of the topological phase of Bi_2Se_3 under mechanical strain

Steve M. Young,¹ Sugata Chowdhury,¹ Eric J. Walter,² Eugene J. Mele,³ Charles L. Kane,³ and Andrew M. Rappe^{1,*}

¹*The Makineni Theoretical Laboratories, Department of Chemistry,
University of Pennsylvania, Philadelphia, PA 19104-6323, USA.*

²*Department of Physics, College of William and Mary, Williamsburg, VA 23187-8795, USA.*

³*Department of Physics, University of Pennsylvania, Philadelphia, PA 19104-6323, USA.*

(Dated: July 21, 2011)

The topological insulating phase results from inversion of the band gap due to spin-orbit coupling at an odd number of time-reversal symmetric points. In Bi_2Se_3 , this inversion occurs at the Γ point. For bulk Bi_2Se_3 , we have analyzed the effect of arbitrary strain on the Γ point band gap using Density Functional Theory. By computing the band structure both with and without spin-orbit interactions, we consider the effects of strain on the gap via Coulombic interaction and spin-orbit interaction separately. While compressive strain acts to decrease the Coulombic gap, it also increases the strength of the spin-orbit interaction, increasing the inverted gap. Comparison with Bi_2Te_3 supports the conclusion that effects on both Coulombic and spin-orbit interactions are critical to understanding the behavior of topological insulators under strain, and we propose that the topological insulating phase can be effectively manipulated by inducing strain through chemical substitution.

PACS numbers: 03.65.Vf, 71.30.+h, 62.20.-x, 64.70.-p,

I. INTRODUCTION

The discovery of the topological insulating (TI) phase of materials has garnered intense interest from the condensed matter physics community and spawned numerous investigations to explore the nature of its origins and effects.^{1–6} These materials have an insulating gap in the bulk, while also possessing conducting, gapless edge or surface states that are protected by time-reversal symmetry. The prediction and observation of this phase have been made in real materials,^{7–13} reinforcing its status as a topic of interest and importance. While most investigations have focused on fundamental physical properties, the unique properties of the topological insulating phase suggest several practical applications, including spintronics and quantum computation.^{14–17} However, significant progress towards technological applications will require deep understanding of the dependence of the fundamental physics on material structure and composition. In this work, we investigate the relationship between the topological insulating phase and the elastic properties of bismuth selenide. Bi_2Se_3 is chemically stable, easy to synthesize, and exhibits a robust topological phase. Combined with the existing theoretical and experimental studies,^{11,12,18–24} it has emerged as the prototypical topological insulator, and is a natural choice for a preliminary investigation. There has been some interest in the effect of mechanical strain on topological effects,^{25,26} but to our knowledge no systematic investigation has been performed. Here we use *ab initio* methods to evaluate the elastic properties of Bi_2Se_3 , and to connect these to the properties of the topological insulating phase.

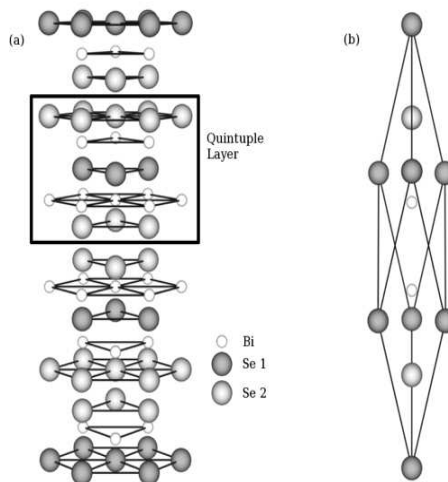


FIG. 1. **Crystal Structure of Bi_2Se_3** : (a) The rhombohedral crystal structure of Bi_2Se_3 consists of hexagonal planes of Bi and Se stacked on top of each other along the z -direction. A quintuple layer with Se1-Bi-Se2-Bi-Se1 is indicated by the black square, where (1) and (2) refer to different lattice positions. (b) Rhombohedral unit cell of Bi_2Se_3 .

II. METHODOLOGY

Density functional theory calculations were performed using the Perdew-Burke-Ernzerhof-type²⁷ generalized gradient approximation (GGA) implemented in the Quantum-Espresso²⁸ code. All atoms are represented by norm-conserving, optimized, designed nonlocal^{29,30} pseudopotentials generated using the OPIUM package.³¹ Pseudopotentials were constructed with and without spin-orbit coupling. All calculations are performed with a plane-wave cutoff of 50 Ry on an $8 \times 8 \times 8$ Monkhorst-Pack³² k-point mesh. The lattice parameters were taken from experiments ($a = 4.138 \text{ \AA}$ and $c = 28.64 \text{ \AA}$).³³ We calculated band structures along the high symmetry lines in the Brillouin-zone (BZ). After fixing the lattice parameters to their experimental values, the atomic coordinates were relaxed to generate the reference structure. It should be noted that the calculations give significant, nonzero stress for the crystal in this geometry.

Various strains were applied relative to the reference structure, including positive and negative uniaxial and shear strains up to 2%, as well as several combinations thereof. The atomic lattice coordinates were relaxed for each strain configuration, and the total and band gap energies were computed both with and without spin-orbit coupling. Multiple regression analysis was performed to find the linear and quadratic dependence of the energy on strain tensor components. This yielded the elastic stiffness and stress tensors.

It is known that in bismuth selenide the topological index distinguishing ordinary insulating from topological insulating behavior is controlled by band inversion at the Γ point. Thus, a band gap stress σ^Γ and band gap stiffness c^Γ were defined as the linear and quadratic coefficients relating the Γ point band gap to strain, by the same procedure used to determine the elastic tensors.

$$\Delta E_g^\Gamma(\epsilon) = \frac{1}{2}c_{ijkl}^\Gamma \epsilon_{ij}\epsilon_{kl} + \sigma_{ij}^\Gamma(0)\epsilon_{ij} \quad (1)$$

In both cases, only the tensor elements unique under the symmetry operations of the space group of bismuth selenide ($R\bar{3}m$, No. 166) were allowed as degrees of freedom. The stiffness and stress tensors, in Voigt notation, must have the forms

$$c = \begin{bmatrix} c_{11} & c_{12} & c_{13} & c_{14} & 0 & 0 \\ c_{12} & c_{11} & c_{13} & -c_{14} & 0 & 0 \\ c_{13} & c_{13} & c_{33} & 0 & 0 & 0 \\ c_{14} & -c_{14} & 0 & c_{44} & 0 & 0 \\ 0 & 0 & 0 & 0 & c_{44} & c_{14} \\ 0 & 0 & 0 & 0 & c_{14} & c_{66} \end{bmatrix}, \quad \sigma = \begin{bmatrix} \sigma_1 \\ \sigma_1 \\ \sigma_3 \\ 0 \\ 0 \\ 0 \end{bmatrix} \quad (2)$$

III. RESULTS AND DISCUSSION

The bulk crystal structure of Bi_2Se_3 is rhombohedral with space group D_{3d}^5 ($R\bar{3}m$, No. 166)³³, shown in Fig. 1. The primitive unit cell has two Bi and three Se atoms, and the atomic plane arrangement is Se(1)-Bi-Se(2)-Bi-Se(1), where Se(1) and Se(2) indicate the two different types of selenium atom in the crystal. In the hexagonal supercell, the structure can be described as quintuple layers (QL) (square region in Fig. 1 of atoms stacked along the trigonal axis (three-fold rotational axis)).

The band structure of Bi_2Se_3 and related compounds have been theoretically predicted^{12,13,34,35} and experimentally

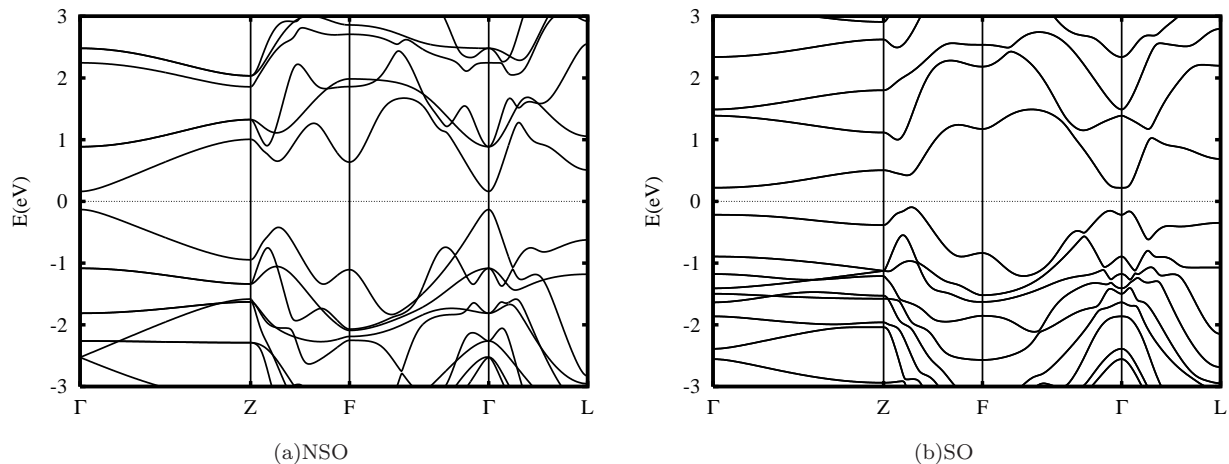


FIG. 2. Band structure in the reference strain state of Bi_2Se_3 (a) excluding (NSO) and (b) including (SO) spin-orbit effects. The dashed line indicates the Fermi level.

observed.^{10,11} In our calculations, the band gap of the unrelaxed, experimental structure of Bi_2Se_3 is 0.3 eV, which is consistent with the experimental data and other calculations.^{10,18,19} Fig. 2 shows the band structure with and without spin-orbit interaction, and both are in excellent agreement with previous results.¹³ The computed elastic and band gap tensor components are given in Table I and Table II, respectively. First, we note that the gap stress shown in Table II for strain normal to the plane of the quintuple layers (σ_3^Γ) is much higher than for strain in the plane (σ_1^Γ), which is consistent with the notion that inter-layer interactions are more important in determining the band gap than intra-layer interactions. Second, we observe the change in sign of σ^Γ when spin-orbit interactions are turned off or on. This is to be expected because the spin orbit interaction leads to an inversion of the conduction and valence bands. Thus, strain reduces the bandgap for the trivial (un-inverted) phase and increases the gap for the topological (inverted) phase. Third, the magnitude of the gap stress is larger when spin-orbit interactions are present. From a tight-binding perspective, compressive strain not only strengthens the Coulombic interaction between sites,

Element	Coefficient (GPa)
c_{11}	91.8 ± 1.0
c_{33}	57.4 ± 1.4
c_{44}	45.8 ± 1.0
c_{66}	56.2 ± 1.8
c_{12}	36.6 ± 1.2
c_{13}	38.6 ± 2.0
c_{14}	24.2 ± 1.8
σ_1	-3.447 ± 0.007
σ_3	-1.977 ± 0.010

TABLE I. The unique elements of the elastic stiffness and stress tensors of Bi_2Se_3 . Spin-orbit coupling has been included.

Element	NSO	SO
	Coefficient (eV)	Coefficient (eV)
c_{11}^Γ	-67.8 ± 2.6	35.4 ± 5.6
c_{33}^Γ	55.4 ± 3.6	-60.1 ± 7.6
c_{44}^Γ	-58.0 ± 2.6	23.4 ± 5.6
c_{66}^Γ	-126.6 ± 4.4	69.4 ± 9.6
c_{12}^Γ	60.2 ± 3.2	-33.8 ± 6.8
c_{13}^Γ	6.4 ± 4.2	-12.6 ± 10.8
c_{14}^Γ	-70.0 ± 4.2	45.6 ± 9.0
σ_1^Γ	0.16 ± 0.017	-1.67 ± 0.037
σ_3^Γ	4.33 ± 0.023	-5.27 ± 0.051

TABLE II. The unique elements of the Γ band gap stiffness and stress tensors excluding (NSO) or including (SO) spin-orbit coupling

increasing the associated hopping coefficient and reducing the conventional gap, but also magnifies the spin-orbit effect and its hopping coefficient, increasing the topological gap. Thus, comparing the gap stress with and without spin-orbit interactions provides some insight into the effects of strain on the essential physics of the system.

Using the above tensors, we can predict that the topological phase transition will occur at 6.4% uniaxial strain in the $\langle 111 \rangle$ direction. In Fig. 3, the onset of the topological insulating phase at 7% strain can be observed through changes in the band structure as strain increases. At the transition point, the Dirac cone characteristic of the phase transition is distinctly observable. Of course, such strains are difficult to achieve experimentally. According to the computed elastic tensors, around 2 GPa of uniaxial tensile stress would be required to drive the phase transition, well past the yield stress. However, large strains may be possible by introducing internal stress through chemical substitution.

Bi_2Te_3 is a very similar compound to Bi_2Se_3 , differing only in substitution of the larger tellurium in place of selenium,

	Bi_2Se_3 (reference)	Bi_2Se_3 (strained)	Bi_2Te_3 (reference)
Lattice parameters(Å)	$a = 4.138, c = 28.64$	$a = 4.358, c = 30.46$	$a = 4.358, c = 30.46$
Anion radius (Å)	1.98	1.98	2.21
NSO Gap (eV)	0.02	0.31	0.20
SO Gap (eV)	0.42	-0.06	0.63

TABLE III. Comparison of reference Bi_2Se_3 , Bi_2Se_3 strained to match reference Bi_2Se_3 lattice, and reference Bi_2Te_3 . Spin-Orbit(SO) and Non-Spin-Orbit(NSO) Γ point gaps for all three structures are calculated.

which increases the size of the lattice by about 6%. It is also a topological insulator with band inversion occurring at the Γ point. Given the similarity, one may ask if it is reasonable to view Bi_2Te_3 as intrinsically strained Bi_2Se_3 . To test this hypothesis, we performed a comparison of Bi_2Te_3 to strained Bi_2Se_3 .

In order to generate an appropriate reference structure for comparison, Bi_2Te_3 was relaxed under identical external stress as the reference Bi_2Se_3 (this is labeled “ Bi_2Te_3 (reference)”). The results are shown in Table III. The computed lattice parameters of Bi_2Te_3 are in good agreement with experiment. The Bi_2Se_3 lattice was then strained so that the lattice parameters match that of reference Bi_2Te_3 (this is labeled “ Bi_2Se_3 (strained)”). Using the gap stiffness and

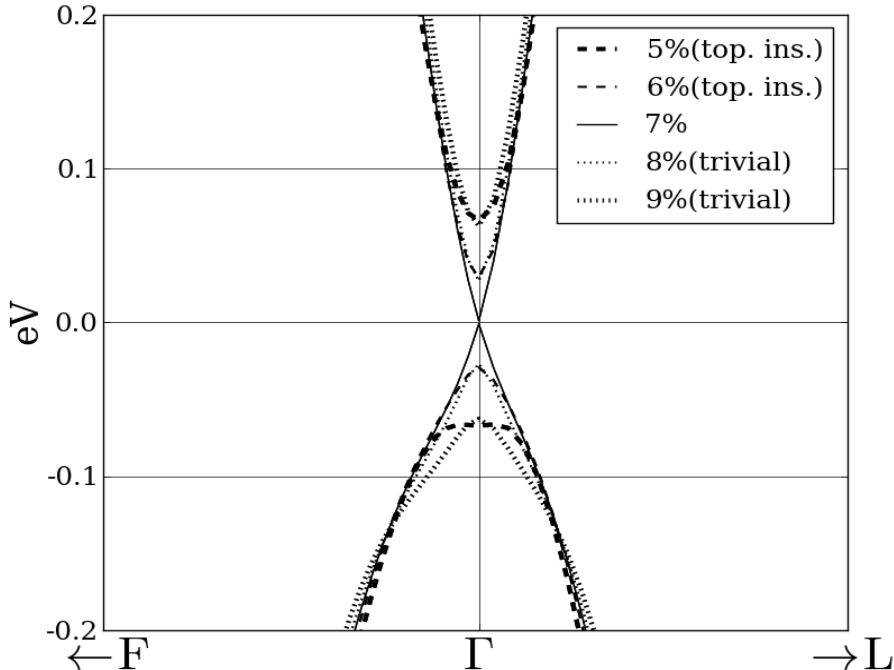


FIG. 3. Band structure of Bi₂Se₃ near the Γ point as $\langle 111 \rangle$ uniaxial strain from 5% to 9% drives the topological phase transition.

stress tensors, the band gap of this strained Bi₂Se₃ was calculated and compared to the computed band gap of Bi₂Te₃. Without spin-orbit interaction, the strained Bi₂Se₃ band gap is similar to the band gap of reference Bi₂Te₃. However, with spin-orbit interaction turned on, the gaps are dramatically different: in the strained Bi₂Se₃, the topological gap closes, but in Bi₂Te₃ the topological gap is quite large. This suggests that spin-orbit effects are strongly dependent on the chemical identity of the anion, and that treating Bi₂Te₃ as strained Bi₂Se₃ fails to capture the essential physics.

IV. CONCLUSION

We have shown that strain is an important parameter for influencing the topological insulating phase. For bismuth selenide, the direct band gap at the gamma point, where band inversion occurs, responds to elastic deformation in a way that can be described by adapting the formalism of continuum mechanics. The critical strain at which the topological phase transition occurs was predicted using the derived band gap stress and stiffness tensors and observed in the computed band structure as a Dirac cone. While it may be possible to tune the band gap with external stress, more interesting is the potential for inducing strain via chemical substitution. Viewing bismuth telluride as chemically strained bismuth selenide, however, fails dramatically, hinting at a complex relationship between chemical composition, material structure, and the physics underlying the topological insulating phase.

V. ACKNOWLEDGMENT

SMY was supported by the Department of Energy Office of Basic Energy Sciences, under Grant No. DE-FG02-07ER46431. SC acknowledges the support of the National Science Foundation, through the MRSEC program, Grant No. DMR05-20020, as well as computational support from the Center for Piezoelectrics by Design. AMR acknowledges the support of the Office of Naval Research, under Grant No. N-000014-00-1-0372, as well as computational support from the HPCMO. C.L.K. acknowledges support from NSF grant DMR-0906175. EJM was supported by the Department of Energy under Grant No. DE-FG02-ER45118.

-
- * rappe@sas.upenn.edu
- ¹ C. L. Kane and E. J. Mele, Phys. Rev. Lett. **95**, 226801 (Nov. 2005).
 - ² C. L. Kane and E. J. Mele, Phys. Rev. Lett. **95**, 146802 (2005).
 - ³ L. Fu, C. L. Kane, and E. J. Mele, Phys. Rev. Lett. **98**, 106803 (2007).
 - ⁴ J. E. Moore and L. Balents, Phys. Rev. B **75**, 121306 (Mar. 2007).
 - ⁵ R. Roy, Phys. Rev. B **79**, 195322 (May 2009).
 - ⁶ M. Z. Hasan and C. L. Kane, Rev. Mod. Phys. **82**, 3045 (Nov. 2010).
 - ⁷ B. A. Bernevig, T. L. Hughes, and S.-C. Zhang, Science **314**, 1757 (2006).
 - ⁸ L. Fu and C. L. Kane, Phys. Rev. B **76**, 045302 (Jul. 2007).
 - ⁹ M. König, S. Wiedmann, C. Brune, A. Roth, H. Buhmann, L. W. Molenkamp, X. L. Qi, and S. C. Zhang, Science **318**, 766 (Nov. 2007).
 - ¹⁰ D. Hsieh, D. Qian, L. Wray, Y. Xia, Y. S. Hor, R. J. Cava, and M. Z. Hasan, Nature **452**, 970 (Apr. 2008).
 - ¹¹ Y. L. Chen, J. G. Analytis, J. H. Chu, Z. K. Liu, S. K. Mo, X. L. Qi, H. J. Zhang, D. H. Lu, X. Dai, Z. Fang, S. C. Zhang, I. R. Fisher, Z. Hussain, and Z. X. Shen, Science **325**, 178 (Jul. 2009).
 - ¹² Y. Xia, D. Qian, D. Hsieh, L. Wray, A. Pal, H. Lin, A. Bansil, D. Grauer, Y. S. Hor, R. J. Cava, and M. Z. Hasan, Nat. Phys. **5**, 398 (Jun. 2009).
 - ¹³ H. J. Zhang, C. X. Liu, X. L. Qi, X. Dai, Z. Fang, and S. C. Zhang, Nat. Phys. **5**, 438 (Jun. 2009).
 - ¹⁴ L. Fu and C. L. Kane, Phys. Rev. Lett. **100**, 096407 (Mar. 2008).
 - ¹⁵ X. L. Qi, T. L. Hughes, and S. C. Zhang, Phys. Rev. B **78**, 195424 (Nov. 2008).
 - ¹⁶ X. L. Qi, R. D. Li, J. D. Zang, and S. C. Zhang, Science **323**, 1184 (Feb. 2009).
 - ¹⁷ A. M. Essin, J. E. Moore, and D. Vanderbilt, Phys. Rev. Lett. **102**, 146805 (Apr. 2009).
 - ¹⁸ E. Mooser and W. B. Pearson, Phys. Rev. **101**, 492 (1956).
 - ¹⁹ J. Black, E. M. Conwell, L. Seigle, and C. W. Spencer, J. Phys. Chem. Solids **2**, 240 (1957).
 - ²⁰ G. H. Zhang, H. J. Qin, J. Teng, J. D. Guo, Q. L. Guo, X. Dai, Z. Fang, and K. H. Wu, Appl. Phys. Lett. **95**, 053114 (Aug. 2009).
 - ²¹ H. L. Peng, K. J. Lai, D. S. Kong, S. Meister, Y. L. Chen, X. L. Qi, S. C. Zhang, Z. X. Shen, and Y. Cui, Nat. Mater. **9**, 225 (Mar. 2010).
 - ²² Y. Li, G. Wang, X. Zhu, M. Liu, C. Ye, X. Chen, Y. Wang, K. He, L. Wang, X. Ma, H. Zhang, X. Dai, Z. Fang, X. Xie, Y. Liu, X. Qi, J. Jia, S. Zhang, and Q. Xue, ArXiv e-prints(Dec. 2009), arXiv:0912.5054 [cond-mat.mes-hall].
 - ²³ Y. Zhang, K. He, C. Z. Chang, C. L. Song, L. L. Wang, X. Chen, J. F. Jia, Z. Fang, X. Dai, W. Y. Shan, S. Q. Shen, Q. Niu, X. L. Qi, S. C. Zhang, X. C. Ma, and Q. K. Xue, Nat. Phys. **6**, 584 (Aug. 2010).
 - ²⁴ T. Zhang, P. Cheng, X. Chen, J. F. Jia, X. C. Ma, K. He, L. L. Wang, H. J. Zhang, X. Dai, Z. Fang, X. C. Xie, and Q. K. Xue, Phys. Rev. Lett. **103**, 266803 (Dec. 2009).
 - ²⁵ J. L. Zhang, S. J. Zhang, H. M. Weng, W. Zhang, L. X. Yang, Q. Q. Liu, S. M. Feng, X. C. Wang, R. C. Yu, L. Z. Cao, L. Wang, W. G. Yang, H. Z. Liu, W. Y. Zhao, S. C. Zhang, X. Dai, Z. Fang, and C. Q. Jin, Proc. Natl. Acad. Sci. **108**, 24 (2011), <http://www.pnas.org/content/108/1/24.full.pdf+html>, <http://www.pnas.org/content/108/1/24.abstract>.
 - ²⁶ C. Brüne, C. X. Liu, E. G. Novik, E. M. Hankiewicz, H. Buhmann, Y. L. Chen, X. L. Qi, Z. X. Shen, S. C. Zhang, and L. W. Molenkamp, ArXiv e-prints(Jan. 2011), arXiv:1101.2627 [cond-mat.mes-hall].
 - ²⁷ J. P. Perdew, K. Burke, and M. Ernzerhof, Phys. Rev. Lett. **77**, 3865 (1996).
 - ²⁸ P. Giannozzi, S. Baroni, N. Bonini, M. Calandra, R. Car, C. Cavazzoni, D. Ceresoli, G. L. Chiarotti, M. Cococcioni, I. Dabo, A. D. Corso, S. de Gironcoli, S. Fabris, G. Fratesi, R. Gebauer, U. Gerstmann, C. Gougoussis, A. Kokalj, M. Lazzeri, L. Martin-Samos, N. Marzari, F. Mauri, R. Mazzarello, S. Paolini, A. Pasquarello, L. Paulatto, C. Sbraccia, S. Scandolo, G. Sclauzero, A. P. Seitsonen, A. Smogunov, P. Umari, and R. M. Wentzcovitch, J. Phys.:Condens. Matter **21**, 395502 (2009).
 - ²⁹ N. J. Ramer and A. M. Rappe, Phys. Rev. B **59**, 12471 (1999).
 - ³⁰ A. M. Rappe, K. M. Rabe, E. Kaxiras, and J. D. Joannopoulos, Phys. Rev. B Rapid Comm. **41**, 1227 (1990).
 - ³¹ <http://opium.sourceforge.net>.
 - ³² H. J. Monkhorst and J. D. Pack, Phys. Rev. B **13**, 5188 (1976).
 - ³³ J. R. Wiese and L. Muldrew, J. Phys. Chem. Solids **15**, 13 (1960).
 - ³⁴ S. K. Mishra, S. Satpathy, and O. Jepsen, Journal of Physics-condensed Matter **9**, 461 (Jan. 1997).
 - ³⁵ W. Zhang, R. Yu, H. J. Zhang, X. Dai, and Z. Fang, New J. Phys. **12**, 065013 (Jun. 2010).